

Dynamical behavior of memristor-coupled heterogeneous discrete neural networks with synaptic crosstalk

Minglin Ma(马铭磷), Kangling Xiong(熊康灵), Zhijun Li(李志军), and Shaobo He(贺少波)

Citation: Chin. Phys. B, 2024, 33 (**2**): 028706. DOI: 10.1088/1674-1056/aceee9
Journal homepage: http://cpb.iphy.ac.cn; http://iopscience.iop.org/cpb

What follows is a list of articles you may be interested in

Dynamics and synchronization in a memristor-coupled discrete heterogeneous neuron network considering noise

Xun Yan(晏询), Zhijun Li(李志军), and Chunlai Li(李春来)
Chin. Phys. B, 2024, 33 (**2**): 028705. DOI: 10.1088/1674-1056/ad062c

Synchronization coexistence in a Rulkov neural network based on locally active discrete memristor

Ming-Lin Ma(马铭磷), Xiao-Hua Xie(谢小华), Yang Yang(杨阳), Zhi-Jun Li(李志军), and Yi-Chuang Sun(孙义闯)
Chin. Phys. B, 2023, 32 (**5**): 058701. DOI: 10.1088/1674-1056/acb9f7

Hopf bifurcation and phase synchronization in memristor-coupled Hindmarsh-Rose and FitzHugh-Nagumo neurons with two time delays

Zhan-Hong Guo(郭展宏), Zhi-Jun Li(李志军), Meng-Jiao Wang(王梦蛟), and Ming-Lin Ma(马铭磷)
Chin. Phys. B, 2023, 32 (**3**): 038701. DOI: 10.1088/1674-1056/aca601

Cross-frequency network analysis of functional brain connectivity in temporal lobe epilepsy

Hai-Tao Yu(于海涛), Li-Hui Cai(蔡立辉), Xin-Yu Wu(武欣昱), Jiang Wang(王江), Jing Liu(刘静), Hong Zhang(张宏)
Chin. Phys. B, 2019, 28 (**4**): 048702. DOI: 10.1088/1674-1056/28/4/048702

Bursting synchronization in clustered neuronal networks

Yu Hai-Tao (于海涛), Wang Jiang (王江), Deng Bin (邓斌), Wei Xi-Le (魏熙乐)
Chin. Phys. B, 2013, 22 (**1**): 018701. DOI: 10.1088/1674-1056/22/1/018701

Dynamical behavior of memristor-coupled heterogeneous discrete neural networks with synaptic crosstalk

Minglin Ma(马铭磷)†, Kangling Xiong(熊康灵), Zhijun Li(李志军), and Shaobo He(贺少波)

School of Automation and Electronic Information, Xiangtan University, Xiangtan 411105, *China*

(Received 1 July 2023; revised manuscript received 23 July 2023; accepted manuscript online 10 August 2023)

Synaptic crosstalk is a prevalent phenomenon among neuronal synapses, playing a crucial role in the transmission of neural signals. Therefore, considering synaptic crosstalk behavior and investigating the dynamical behavior of discrete neural networks are highly necessary. In this paper, we propose a heterogeneous discrete neural network (HDNN) consisting of a three-dimensional KTz discrete neuron and a Chialvo discrete neuron. These two neurons are coupled mutually by two discrete memristors and the synaptic crosstalk is considered. The impact of crosstalk strength on the firing behavior of the HDNN is explored through bifurcation diagrams and Lyapunov exponents. It is observed that the HDNN exhibits different coexisting attractors under varying crosstalk strengths. Furthermore, the influence of different crosstalk strengths on the synchronized firing of the HDNN is investigated, revealing a gradual attainment of phase synchronization between the two discrete neurons as the crosstalk strength decreases.

Keywords: discrete memristor, synaptic crosstalk, coexisting attractor, phase synchronization

PACS: 87.19.lg, 87.19.lj ,87.19.lm, 45.05.+x **DOI:** 10.1088/1674-1056/aceee9

1. Introduction

Neurons are the fundamental units of structure and function in the nervous system, and they form neural networks through various types of connections.[1] Neural networks play a crucial role in fields such as signal processing,[2,3] associative memory,[4,5] robot control,[6] and image processing.[7–9] As is widely known, a memristor is a device that describes the relationship between charge and flux.[10] Since its development by HP Laboratory in 2008, memristors have found extensive applications in neural networks,[11–15] image encryption,[16,17] chaotic systems,[18–24] and more. Due to their unique biomimetic properties, such as nanoscale size, low power consumption, and non-volatility, continuous memristors are considered the optimal choice for simulating synapses in analog form.[25–30] Compared to conventional electronic synapses, neural networks based on memristive synapses can more effectively mimic the complex firing activity of biological neural networks. For instance, memristor-coupled neural networks can generate grid multi-scroll attractors,[31–34] diverse chaotic attractors that are employed in image encryption.[35] Locally active memristor-based Hopfield neural networks can exhibit more complex dynamical behaviors.[36]

So far, several models of discrete neurons, such as the Chialvo model, Rulkov model, Izhikevich model, and Kinouvhi and Tragtenberg (KT) model, have been proposed. Discrete neuron models have advantages over continuous neuron models in terms of computational time, computational resources, and data storage.[37–42] Therefore, discrete neuron models are more suitable for simulating large-scale neural networks and conducting general research, such as generating chaotic trajectories, pattern recognition, and analyzing synchronized firing behaviors.[43–51] As a result, research on discrete neurons has become a hot topic in recent years. In discrete memristor-coupled neural networks, complex dynamical behaviors have been discovered, including coexisting attractors,[52–56] synchronization transitions, and synchronization coexistence.[57,58] Additionally, Lu *et al.*[59] investigated fractional-order neural networks based on discrete memristors and found that this system exhibits richer dynamical behaviors compared to integer-order neural networks.

Synaptic crosstalk refers to the spillover of neurotransmitters from one synapse to another or the lateral diffusion of receptors from one spine to neighboring spines. It has profound implications for neural signal transmission.[60,61] Increasing evidence suggests the widespread occurrence of synaptic crosstalk among neuronal synapses. Considering synaptic crosstalk, Leng *et al.* proposed a heterogeneous neural network (HNN) and analyzed the dynamical behavior of the HNN.[62] Li *et al.* proposed an associative memory circuit based on memristors that takes into account synaptic crosstalk and demonstrated its impact on memory function.[63] Based on the above research, we found that crosstalk can affect the dynamic behavior and associative memory energy of neural networks. Therefore, exploring the behavior of discrete neural networks with crosstalk behavior has practical significance.

Inspired by the aforementioned papers, it is proposed that discrete memristors are used to mimic synapses, coupling a Chialvo neuron and a KTz neuron. Considering the crosstalk behavior between synapses, a memristor-coupled

†Corresponding author. E-mail: minglin_ma@xtu.edu.cn

© 2024 Chinese Physical Society and IOP Publishing Ltd

HDNN model is constructed and the dynamical behavior of this neural network is analyzed. The structure of this paper is as follows: In Section 2, a novel discrete memristor model is introduced. In Section 3, the memristor-coupled HDNN model with synaptic crosstalk is proposed. Section 4 investigates the coexistence behavior of the HDNN. In Section 5, the phase synchronization behavior of the memristor-coupled HDNN under different crosstalk strengths is discussed. Finally, conclusions are provided.

2. Discrete memristor

2.1. Discrete memristor model and its characteristics

In this study, we employ two discrete memristors to mimic synapses, coupling two different types of neurons: a KTz neuron and a Chialvo neuron. The topological structure of this neural network is illustrated in Fig. 1. The model of the memristor synapse can be expressed by

$$\begin{cases} i(n) = W[q(n)]\,v(n) = \tanh(q(n))v(n), \\ q(n+1) = F(q,v) \\ \qquad = q(n) + \alpha(q(n)(\delta - \gamma|q(n)|)) + \alpha\beta v(n), \end{cases} \tag{1}$$

where $i(n)$ and $v(n)$ respectively represent the input current and voltage at both ends of the discrete memristor, and $W[q(n)]$ is the memristor inductance value of the memristor. α, γ, δ, β are four memristor parameters. In this paper, we set $\alpha = 0.1$, $\beta = 1$, $\delta = 5$, $\gamma = 1$. To model the phenomenon of synaptic crosstalk, we consider the interaction between two memristors. The weights of the two discrete memristor synapses can be described as follows:

$$\begin{cases} W_1(q_1(n), q_2(n)) = W_1(q_1(n)) + b_1 W_2(q_2(n)), \\ W_2(q_2(n), q_1(n)) = W_2(q_2(n)) + b_2 W_1(q_1(n)), \end{cases} \tag{2}$$

where $W_1(q_1(n))$ and $W_2(q_2(n))$ represent the weights of synapse_1 and synapse_2, respectively, without considering crosstalk. $W_1(q_1(n), q_2(n))$ and $W_2(q_1(n), q_2(n))$ represent the weights of synapse_1 and synapse_2, respectively, when considering crosstalk. b_1 and b_2 are the crosstalk intensities, where $b_1 W_2(q_2(n))$ represents the influence of synapse_2 on synapse_1, and $b_2 W_1(q_1(n))$ represents the influence of synapse_1 on synapse_2.

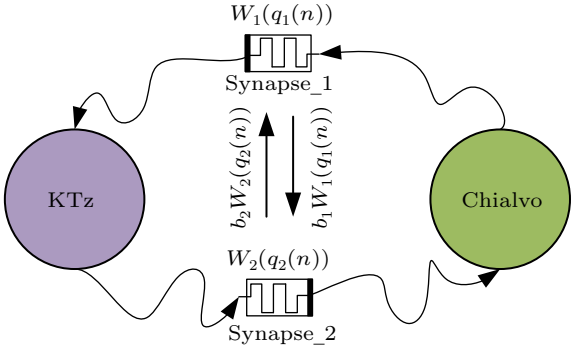


Fig. 1. Topological structure of the HDNN with synaptic crosstalk.

2.2. Pinched hysteresis loops

Under the condition of an input sinusoidal voltage signal $v(n) = A\sin(wT(n))$, and the initial value of the discrete memristor $q(1) = -2$, the voltage–current characteristic curve of the discrete memristor is shown in Fig. 2. By changing the amplitude of the sinusoidal voltage signal, figure 2(a) illustrates an "8" shaped hysteresis loop crossing the origin, and the area of the loop gradually increases with the increase in amplitude. By varying the frequency of the sinusoidal voltage signal, figure 2(b) shows the hysteresis loop gradually shrinking. As the frequency increases, the area of the hysteresis loop gradually decreases until it becomes a single-valued function. Therefore, this discrete memristor complies with the definition of a generalized memristor.

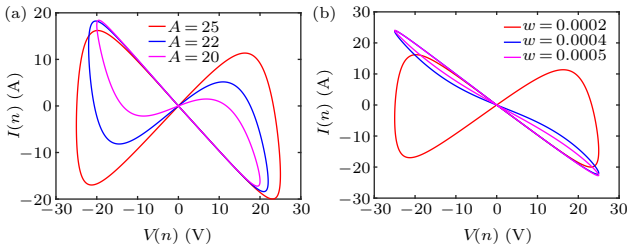


Fig. 2. Hysteresis loop of the memristor: (a) $w = 0.0002$, $A = 20, 22, 25$, (b) $A = 25$, $w = 0.0002, 0.0004, 0.0005$.

3. Memristor-coupled HDNN

3.1. KTz neurons and Chialvo neurons

The model of three-dimensional KTz neurons is as follows:[64]

$$\begin{cases} x(n+1) = \tanh\left(\frac{x(n) - ay(n) + z(n) + d}{t}\right), \\ y(n+1) = x(n), \\ z(n+1) = (1-g)z(n) - h(x(n) - u), \end{cases} \tag{3}$$

where $x(n)$ represents the membrane potential of the neuron, $y(n)$ denotes the recovery variable, $z(n)$ represents the slow total ion current. a, d, t, g, h and u are parameters that control the firing patterns of the neuron.

The model of two-dimensional Chialvo neurons is as follows:[65]

$$\begin{cases} x(n+1) = [x(n)]^2 \exp[y(n) - x(n)] + I(t), \\ y(n+1) = ay(n) - bx(n) + c, \end{cases} \tag{4}$$

where $x(n)$ represents the membrane potential of the neuron, $y(n)$ denotes the recovery variable, a, b and c are parameters, and $I(t)$ can be regarded as the external input current.

3.2. Model of the memristor-coupled HDNN

The model of the memristor-coupled HDNN with synaptic crosstalk is represented by Eq. (5), where k is the coupling strength of the neural network, b_1 and b_2 are the crosstalk

strengths of the system. The remaining parameters of the system are as follows: $a = 0.6$, $t = 0.35$, $c = 0.1$, $c_1 = 0.28$, $a_1 = 0.9$, $d = 0.4$, $d_1 = 0.03$, $r = 0.6$, $k = 0.2$, $g = 0.008$, $h = 0.008$, $u = -0.3$, $\delta = 5$, $\gamma = 2$.

$$\begin{cases} x_1(n+1) = \tanh\left(\frac{x_1(n)-ay_1(n)+z_1(n)+d}{t}\right) - k\big(\tanh(q_2(n)) \\ \qquad + b_1\tanh(q_1(n))\big)\,(x_1(n)-x_2(n)), \\ y_1(n+1) = x_1(n), \\ z_1(n+1) = (1-g)z_1(n) - h(x_1(n)-u), \\ x_2(n+1) = [x_2(n)]^2\exp[y_2(n)-x_2(n)] + d_1 \\ \qquad + k\,(\tanh(q_1(n)) + b_2\tanh(q_2(n))) \\ \qquad \times (x_1(n)-x_2(n)), \\ y_2(n+1) = a_1y_2(n) - rx_2(n) + c_1, \\ q_1(n+1) = q_1(n) + c(q_1(n)(\delta - \gamma|q_1(n)|)) \\ \qquad + c\,(x_2(n)-x_1(n)), \\ q_2(n+1) = q_2(n) + c(q_2(n)(\delta - \gamma|q_2(n)|)) \\ \qquad + c\,(x_1(n)-x_2(n)). \end{cases} \tag{5}$$

3.3. Analysis of equilibrium points

According to Eq. (5), the equilibrium point $E(x_1^{(e)}, y_1^{(e)}, z_1^{(e)}, x_2^{(e)}, y_2^{(e)}, q_1^{(e)}, q_2^{(e)})$ of the system can be obtained as follows:

$$E\left(x_1^{(e)}, x_1^{(e)}, -(x_1^{(e)}+0.3), x_2^{(e)}, -6x_2^{(e)}+2.8, q_1^{(e)}, q_2^{(e)}\right). \tag{6}$$

According to Eqs. (5) and (6), the following equation can be derived:

$$\begin{cases} x_1^{(e)} - \tanh\left(\frac{-12x_1^{(e)}+2}{7}\right) \\ +0.2(\tanh(q_2^{(e)}) + b_1\tanh(q_1^{(e)}))(x_1^{(e)} - x_2^{(e)}) = 0, \\ x_2^{(e)} - x_2^{(e)2}\exp\left(-7x_2^{(e)}+2.8\right) - 0.03 \\ -0.2(\tanh(q_1^{(e)}) + b_2\tanh(q_2^{(e)}))(x_1^{(e)} - x_2^{(e)}) = 0, \\ q_1^{(e)}\left(5 - \left|q_1^{(e)}\right|\right) + (x_2^{(e)} - x_1^{(e)}) = 0, \\ q_2^{(e)}\left(5 - \left|q_2^{(e)}\right|\right) + (x_1^{(e)} - x_2^{(e)}) = 0. \end{cases} \tag{7}$$

The corresponding Jacobian matrix is

$$J_e = \begin{bmatrix} A & B & A & C & 0 & -b_1E & F \\ 1 & 0 & 0 & 0 & 0 & 0 & 0 \\ -0.008 & 0 & 0.992 & 0 & 0 & 0 & 0 \\ N & 0 & 0 & M & D & E & -b_2F \\ 0 & 0 & 0 & -0.6 & 0.9 & 0 & 0 \\ -0.1 & 0 & 0 & 0.1 & 0 & V_1 & 0 \\ 0.1 & 0 & 0 & -0.1 & 0 & 0 & V_2 \end{bmatrix}, \tag{8}$$

with

$$A = \frac{20}{7}\left(\operatorname{sech}\frac{x_1^{(e)} - 0.6y_1^{(e)} + z_1^{(e)} + 0.4}{0.35}\right)^2 - C, \tag{9}$$

$$B = -\frac{12}{7}\left(\operatorname{sech}\frac{x_1^{(e)} - 0.6y_1^{(e)} + z_1^{(e)} + 0.4}{0.35}\right)^2, \tag{10}$$

$$C = k(\tanh q_2^{(e)} + b_1\tanh q_1^{(e)}), \tag{11}$$

$$D = \left[x_2^{(e)}\right]^2\exp(y_2^{(e)} - x_2^{(e)}), \tag{12}$$

$$E = k(x_1^{(e)} - x_2^{(e)})(\operatorname{sech} q_1^{(e)})^2, \tag{13}$$

$$F = -k(x_1^{(e)} - x_2^{(e)})(\operatorname{sech} q_2^{(e)})^2, \tag{14}$$

$$M = 2x_2^{(e)}\exp\left(y_2^{(e)} - x_2^{(e)}\right) \tag{15}$$

$$- \left[x_2^{(e)}\right]^2\exp\left(y_2^{(e)} - x_2^{(e)}\right) - N, \tag{16}$$

$$N = k(\tanh q_1^{(e)} + b_2\tanh q_2^{(e)}), \tag{17}$$

$$V_1 = 0.1(5 - \operatorname{abs}(q_1^{(e)})) + q_1^{(e)}(-\operatorname{sign}(q_1^{(e)})), \tag{18}$$

$$V_2 = 0.1(5 - \operatorname{abs}(q_2^{(e)})) + q_2^{(e)}(-\operatorname{sign}(q_2^{(e)})). \tag{19}$$

The eigenvalues of the Jacobian matrix can be obtained by

$$P(\lambda) = \det(\lambda I - J_e). \tag{20}$$

The equilibrium points and eigenvalues for different levels of crosstalk strength are shown in Table 1.

Table 1. Equilibrium points, corresponding eigenvalues and stabilities.

(b_1, b_2)	$(x_1(n), x_2(n), q_1(n), q_2(n))$	Eigenvalues	Stabilities
(0.5, 0.5)	(0.1090, 0.1439, 5.0070, 4.993)	1.6755, 1.0403 ± 0.47i, 1.0672, 0.9021, 0.5014, 0.4986	unstable
	(0.1051, 0.0562, 0.0098, −0.0098)	1.9161, 0.7886, 1.1123, 1.1078, 1.0001, 1.5027, 1.4980	unstable
	(0.1191, −0.007, −5.0251, −4.9746)	0.4714, 0.0713, 0.8332, 0.8995, 0.6204, 0.5051, 0.4950	stable
	(0.1052, 0.1832, −0.01570.0157)	1.9172, 0.7905, 1.1139, 1.1408, 1.2851, 1.4852, 1.4946	unstable
(1, 1)	(0.1084, 0.1532, −0.0090, 4.9910)	1.6369, 1.2258 ± 0.2919i, 1.4892, 1.0624, 0.8737, 0.5018	unstable
	(0.1051, 0.1829, −4.9844, 4.9844)	1.6054 ± 0.1538i, 1.0974 ± 0.0278i, 0.8312, 0.5031, 0.6032	unstable
	(0.0701, 0.3047, −4.9526, −5.0465)	0.5228, 0.8046 ± 0.1242i, 0.9289, 0.6980, 0.5095, 0.4907	stable
	(0.1270, −0.0209, −5.0294, −4.9702)	2.4671, −0.5134, 1.0359, 0.8968, 0.6454, 0.5060, 0.4941	unstable

The stability of equilibrium points in chaotic systems significantly influences the dynamical behavior. The stability of the equilibrium points can be determined based on the eigenvalues. When the eigenvalues lie within the unit circle, the equilibrium points are stable; otherwise, they are unstable.

To analyze the impact of crosstalk strength on the dynamics of the memristor-coupled HDNN, certain system parameters are held constant as follows: $a = 0.6$, $t = 0.35$, $c = 0.1$,

$c_1 = 0.28$, $a_1 = 0.9$, $d = 0.4$, $d_1 = 0.03$, $r = 0.6$, $g = 0.008$, $h = 0.008$, and $u = -0.3$.

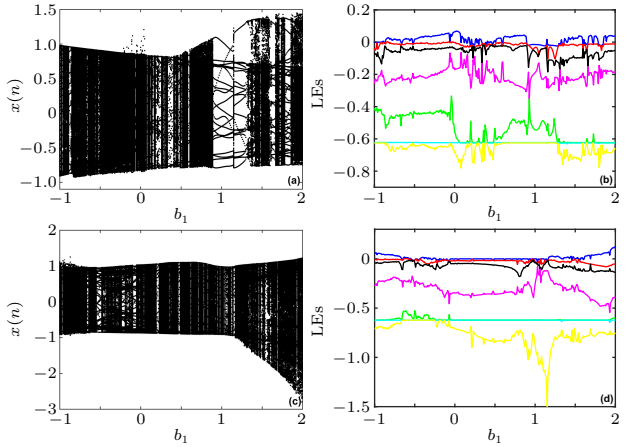


Fig. 3. Bifurcation diagram and Lyapunov exponent plot with respect to crosstalk strength b_1. (a) Bifurcation diagram with respect to b_1 for the initial condition $(-1,1,1,-1,1,1,1)$; (b) Lyapunov exponent plot with respect to b_1 for the initial condition $(-1,1,1,-1,1,1,1)$; (c) bifurcation diagram with respect to b_1 for the initial condition $(-1,1,1,-1,1,-1,1)$; (d) Lyapunov exponent plot with respect to b_1 for the initial condition $(-1,1,1,-1,1,-1,1)$.

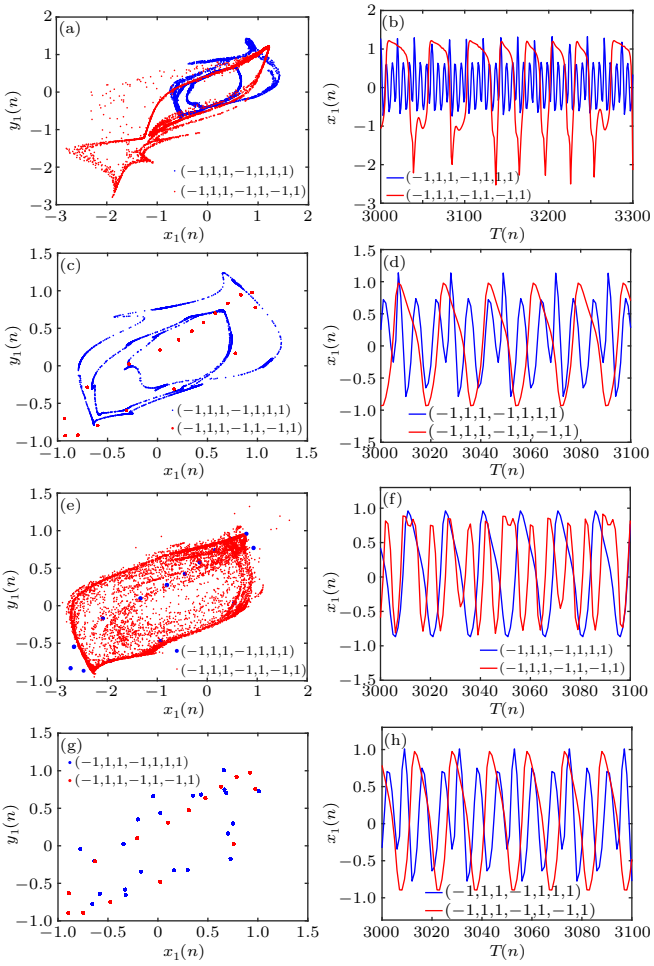


Fig. 4. Phase portrait in the x_1–y_1 plane and time series plot of x_1 for different crosstalk strengths b_1. [(a) and (b)] $b_1 = 2$, coexistence of chaotic attractors and chaotic attractors; [(c) and (d)] $b_1 = 1.15$, coexistence of chaotic attractors and periodic attractors; [(e) and (f)] $b_1 = -0.88$; coexistence of periodic attractors and chaotic attractors; [(g) and (h)] $b_1 = 1.03$, coexistence of periodic attractors and periodic attractors.

4. Impact of crosstalk strength on multistability

4.1. Impact of crosstalk strength b_1

When the coupling strength $k = 0.2$ and the crosstalk strength $b_2 = 0.2$, considering two different initial conditions $(-1,1,1,-1,1,1,1)$ and $(-1,1,1,-1,1,-1,1)$, the bifurcation diagram and Lyapunov exponent plot with respect to the crosstalk strength b_1 are shown in Fig. 3. Obviously, this system shows the characteristics of multistability. To provide a more visual representation of the system's multistability, we plot the different coexisting attractors under different crosstalk strengths in Fig. 4. We observe the coexistence of chaotic attractors with chaotic attractors, chaotic attractors with periodic attractors, periodic attractors with chaotic attractors, and periodic attractors with periodic attractors in the system.

4.2. Impact of crosstalk strength b_2

When the coupling strength $k = 0.2$ and the crosstalk strength $b_1 = 0.85$, considering two different initial conditions $(-1,1,1,-1,1,1,1)$ and $(-1,1,1,-1,1,-1,1)$, the bifurcation diagram and Lyapunov exponent plot with respect to the crosstalk strength b_2 are shown in Fig. 5. Different coexisting attractors under different crosstalk strengths are shown in Fig. 6. It is observed that under this condition, the system exhibits the coexistence of chaotic attractors with chaotic attractors, chaotic attractors with periodic attractors, periodic attractors with chaotic attractors, and periodic attractors with periodic attractors.

5. Impact of crosstalk strength on phase synchronization

When studying the influence of different crosstalk strengths on the phase synchronization of neurons, the phase of the neurons can be expressed by the following equation:

$$\theta(n) = 2\pi \frac{n - n_k}{n_k + 1 - n_k}, \quad (n_k < n < n_k + 1), \tag{21}$$

where n_k represents the occurrence time of the k-th cluster, and n_{k+1} represents the occurrence time of the $(k+1)$ the cluster.

The phase difference between two neurons can be represented by the following equation:

$$|\Delta\theta(n)| = |\theta_1(n) - \theta_2(n)|. \tag{22}$$

With a fixed value of $k = 0.2$ and $b_1 = 0.85$, when the crosstalk strength $b_2 = 0.5$, as shown in Figs. 7(a) and 7(b), the firing pattern of the neurons is characterized by spike firing, and the two neurons are not synchronized. In Figs. 7(c) and 7(d), it can be seen that as the crosstalk strength b_2 decreases to 0.1, the two neurons gradually start to synchronize. When the crosstalk strength $b_2 = -1$, as shown in Figs. 7(e) and 7(f), one neuron exhibits firing in chaotic clusters, while the other neuron exhibits spike firing, and phase synchronization is achieved.

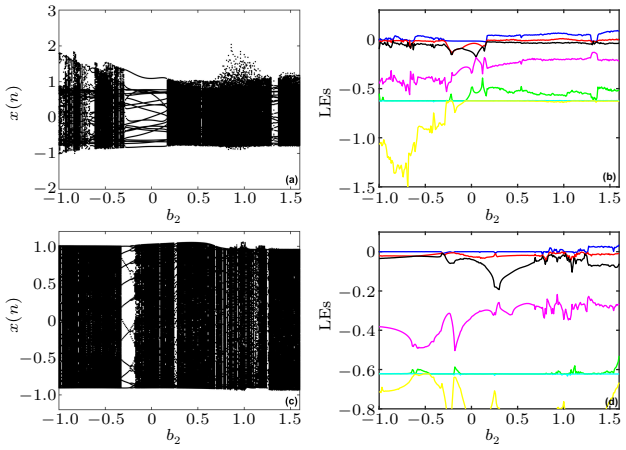


Fig. 5. Bifurcation diagram and Lyapunov exponent plot with respect to crosstalk strength b_2. (a) Bifurcation diagram with respect to b_2 for the initial condition $(-1,1,1,-1,1,1,1)$; (b) Lyapunov exponent plot with respect to b_2 for the initial condition $(-1,1,1,-1,1,1,1)$; (c) bifurcation diagram with respect to b_2 for the initial condition $(-1,1,1,-1,1,-1,1)$; (d) Lyapunov exponent plot with respect to b_2 for the initial condition $(-1,1,1,-1,1,-1,1)$.

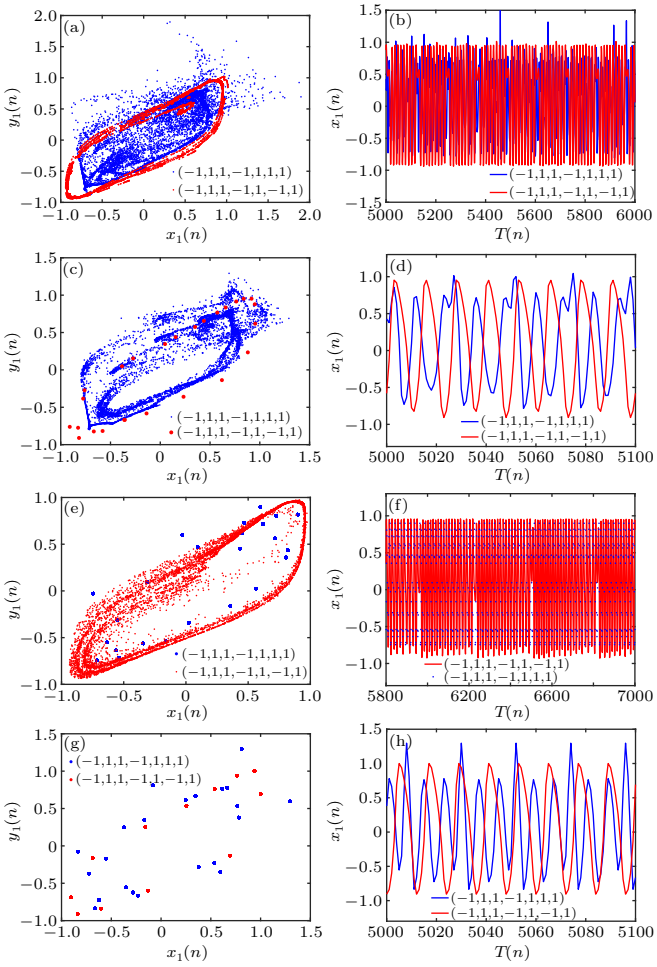


Fig. 6. Phase portrait in the x_1–y_1 plane and time series plot of x_1 for different crosstalk strengths b_2. [(a) and (b)] $b_2 = 1$, coexistence of chaotic attractors and chaotic attractors; [(c) and (d)] $b_2 = 1.255$, coexistence of chaotic attractors and periodic attractors; [(e) and (f)] $b_2 = 1.3$, coexistence of periodic attractors and chaotic attractors; [(g) and (h)] $b_2 = -0.25$, coexistence of periodic attractors and periodic attractors.

With a fixed crosstalk strength of $b_2 = 0.2$, when the crosstalk strength $b_1 = 0.1$, as shown in Figs. 8(a) and 8(b), it can be observed that the phase of the two neurons is not synchronized. As depicted in Figs. 8(c) and 8(d), when the crosstalk strength b_1 decreases to -0.5, their phases gradually synchronize. Further reducing the crosstalk strength to -1.2, both neurons exhibit spike firing patterns and achieve phase synchronization.

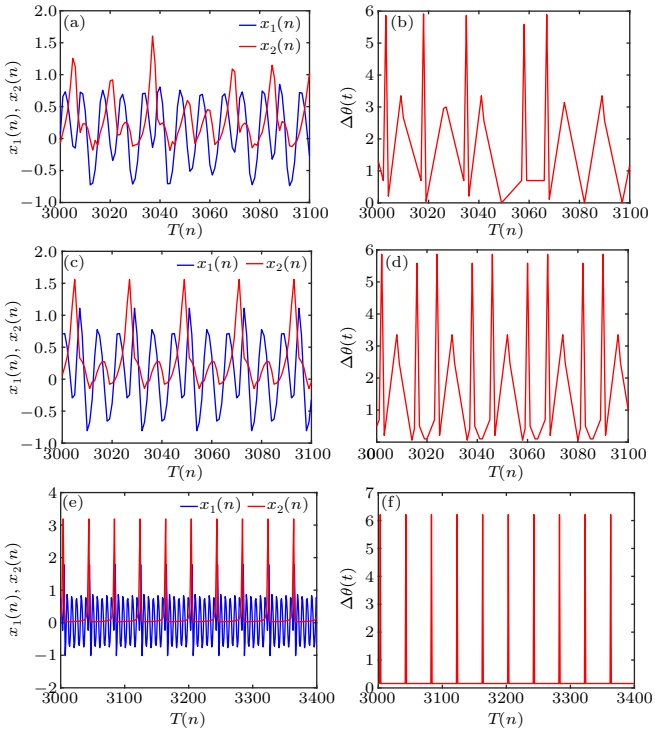


Fig. 7. Synchronization transition of the memristor-coupled HDNN with a fixed crosstalk strength of b_1. [(a) and (b)] $b_2 = 0.5$; [(c) and (d)] $b_2 = 0.1$; [(e) and (f)] $b_2 = -1$.

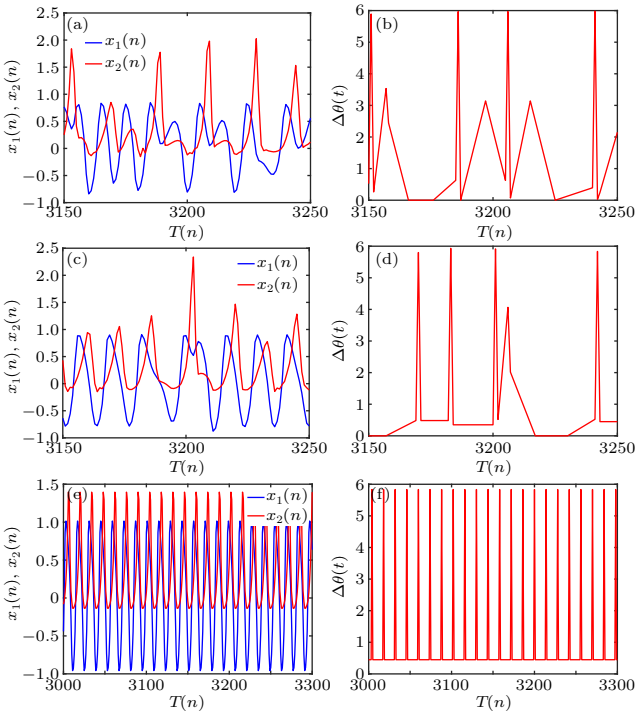


Fig. 8. Synchronization transition of the memristor-coupled HDNN with a fixed crosstalk strength of b_2. [(a) and (b)] b_1 =0; [(c) and (d)] $b_1 = -0.5$; [(e) and (f)] $b_1 = -1.2$.

6. Conclusion

In this paper, we propose a memristor-coupled HDNN, which consists of a two-dimensional Chialvo discrete neuron, a three-dimensional KTz discrete neuron, and two memristor synapses. The synaptic crosstalk within the network is modeled by mutual coupling between the memristor synapses. It is found that the system exhibits different attractor coexistence phenomena under different crosstalk strengths, including coexisting chaotic and chaotic attractors, coexisting chaotic and periodic attractors, and coexisting periodic and periodic attractors, which reveals the multistability behavior of the memristor-coupled HDNN. Furthermore, in this paper, the synchronous firing behavior between two discrete neurons is investigated by varying the crosstalk strength.

Acknowledgments

Project supported by the Key Projects of Hunan Provincial Department of Education (Grant No. 23A0133), the Natural Science Foundation of Hunan Province (Grant No. 2022JJ30572), and the National Natural Science Foundations of China (Grant No. 62171401).

References

[1] Xie Y, Ying X and Jun M 2023 *Nonlinear Dyn.* **111** 11521
[2] Wen Z, Wang C, Deng Q and Lin H 2022 *Nonlinear Dyn.* **110** 3823
[3] Deng Z K, Wang C H, Lin H R and Sun Y C 2022 *IEEE Trans. Comput.-Aided Des. Int. Circuits Syst.*
[4] Sun J, Wang Y, Liu P, Wen S and Wang Y 2022 *IEEE Trans. Cybern.* **53** 3351
[5] Muni S S, Fatoyinbo H O and Ghosh I 2022 *Int. J. Bifurcation Chaos* **32** 2230020
[6] Jin J, Chen W, Chen C, Chen L, Tang Z, Chen L and Zhu C 2022 *IEEE Trans. Indust. Inform.* **19** 8691
[7] Zhou S, Wang X, Zhang Y, Ge B, Wang M and Gao S 2022 *Multimedia Syst.* **28** 95
[8] Yu F, Shen H, Yu Q, Kong X, Sharma P K and Cai S 2022 *IEEE Trans. Netw. Sci. Eng.* **10** 845
[9] Yu F, Xu S, Xiao X, Yao W, Huang Y, Cai S and Li Y 2023 *Integration* **90** 58
[10] Chua L 1971 *IEEE Trans. Circuit Theory* **18** 507
[11] Muni S S and Provata A 2020 *Nonlinear Dyn.* **101** 2509
[12] Chen C, Min F, Zhang Y and Bao H 2023 *Chaos Solitons Fractals* **167** 113068
[13] Muni S S, Njitacke Z, Feudjio C, Fozin T and Awrejcewicz J 2022 *Chaos Theory Appl.* **4** 119
[14] Chen C, Min F, Zhang Y and Bao B 2021 *Nonlinear Dyn.* **106** 2559
[15] Wan Q, Li F, Chen S and Yang Q 2023 *Chaos Solitons Fractals* **169** 113259
[16] Lai Q, Wan Z, Zhang H and Chen G 2022 *IEEE Trans. Neural Netw. Learn. Syst.*
[17] Lin H, Wang C, Cui L, Sun Y, Zhang X and Yao W 2022 *Nonlinear Dyn.* **110** 841
[18] Yu, F, Zhang W, Xiao X, Yao W, Cai S, Zhang J and Li Y 2023 *Mathematics* **11** 701
[19] Gu H, Li C, Li Y, Ge X and Lei T 2023 *Nonlinear Dyn.* **111** 7807
[20] Chen W, Jin J, Chen C, Yu F and Wang C 2022 *Int. J. Bifurcation Chaos* **32** 2250210
[21] Zhang D and Qian Y 2023 *Mathematics* **11** 1690
[22] Li H, Li C and He S 2023 *Int. J. Bifurcation Chaos* **33** 2350032
[23] Peng C, Li Z, Wang M and Ma M 2023 *Nonlinear Dyn.*
[24] Njitacke Tabekoueng Z, Sriram B, Rajagopal K, Kaethikeyan A and Awrejcewicz J 2023 *Chaos* **33** 063153
[25] Njitacke Tabekoueng Z, Shankar Muni S, Fonzin Fozin T, Dolvis Leutcho G and Awrejcewicz J 2022 *Chaos: Interdiscip. J. Nonlinear Sci.* **32** 053114
[26] Njitacke Z T, Awrejcewicz J, Telem A N K, Fozin T F and Kengne J 2022 *IEEE Trans. Circuits Syst. II: Express Briefs* **70** 791
[27] Ma T, Mou J, Yan H and Cao Y 2022 *Euro. Phys. J. Plus* **137** 1135
[28] Xu Q, Liu T, Ding S, Bao H, Li Z and Chen B 2022 *Cognitive Neurodyn.* **17** 755
[29] Wang M, Peng J, Zhang X, Iu H H C and Li Z 2023 *Nonlinear Dyn.*
[30] Hajian D N, Ramadoss J, Natiq H and Parastesh F 2023 *Chin. J. Phys.* **87** 311
[31] Lai Q, Wan Z and Kuate P D K 2022 *IEEE Trans. Circuits Syst. I: Regular Papers* **70** 1324
[32] Lin H, Wang C, Sun Y and Wang T 2022 *IEEE Trans. Circuits Syst. II: Express Briefs* **70** 311
[33] Wang M J and Gu L F 2024 *Chin. Phys. B* **33** 020504
[34] Tang D, Wang C H, Lin H R and Yu F 2023 *Nonlinear Dyn.*
[35] Lin H, Wang C, Xu C, Zhang X and Iu H H 2022 *IEEE Trans. Comput.-Aided Des. Integr. Circuits Syst.* **42** 942
[36] Yu F, Kong X, Mokbel A A M, Yao W and Cai S 2022 *IEEE Trans. Circuits Syst. II: Express Briefs* **70** 326
[37] Xu Y, Li H L, Zhang L, Hu C and Jiang H 2023 *Neural Process. Lett.*
[38] Shang C, He S, Rajagopal K, Wang H and Sun K 2022 *Eur. Phys. J. Spec. Top.* **231** 4065
[39] Ren L, Mou J, Banerjee S and Zhang Y 2023 *Chaos Solitons Fractals* **167** 113024
[40] Yao Z, Sun K and He S 2022 *Nonlinear Dyn.* **110** 1807
[41] Njitacke Z T, Fozin T F, Muni S S, Awrejcewicz J and Kengne J 2022 *AEU-Int. J. Electron. Commun.* **155** 154361
[42] Rulkov N F 2001 *Phys. Rev. Lett.* **86** 183
[43] Ramadoss J, Almatroud O A, Momani S, Pham V T and Thoai V P 2022 *Symmetry* **14** 2110
[44] Ma M L, Yang Y, Qiu Z, Peng Y, Sun Y, Li Z and Wang M 2022 *Nonlinear Dyn.* **107** 2935
[45] Li H, Li C and Du J 2023 *Nonlinear Dyn.* **111** 2895
[46] Yuan F, Xing G and Deng Y 2023 *Chaos Solitons Fractals* **166** 112888
[47] Lai Q, Yang L and Liu Y 2022 *Chaos Solitons Fractals* **165** 112781
[48] Ma M L, Xie X H, Yang Y, Li Z J and Sun Y C 2023 *Chin. Phys. B* **32** 058701
[49] Yuan F, Xing G and Deng Y 2023 *Chaos Solitons Fractals* **166** 112888
[50] He S, Liu J, Wang H and Sun K 2023 *Neurocomputing* **523** 1
[51] Peng Y, Liu J, He S and Sun K 2023 *Chaos Solitons Fractals* **171** 113429
[52] Almatroud O A and Pham V T 2023 *Mathematics* **11** 1319
[53] Kengne L K, Muni S S, Chedjou J C and Kyandoghere K 2022 *Eur. Phys. J. Plus* **137** 848
[54] Li Y, Xiao L, Wei Z and Zhang W 2020 *Eur. Phys. J. Spec. Top.* **229** 953
[55] Li C, Lei T and Liu Z 2022 *Chaos: Interdiscip. J. Nonlinear Sci.* **32** 121104
[56] Li Y, Wei Z, Zhang W, Perc M and Repnik R 2019 *Appl. Math. Comput.* **354** 180
[57] Ma M L, Lu Y, Li Z, Sun Y and Wang C 2023 *Fractal Fractional* **7** 82
[58] Ma M L, Xiong K, Li Z and Sun Y 2023 *Mathematics* **11** 375
[59] Lu Y M, Wang C H, Deng Q L and Xu C 2022 *Chin. Phys. B* **31** 060502
[60] Kawahara M, Kato-Negishi M and Tanaka K 2017 *Metallomics* **9** 619
[61] Shrivastava A N, Triller A and Sieghart W 2011 *Frontiers Cell. Neurosci.* **5** 7
[62] Leng Y, Yu D, Hu Y, Yu S S and Ye Z 2020 *Chaos* **30** 033108
[63] Li Z and Yi Z 2022 *Electron. Lett.* **58** 539
[64] Chialvo D R 1995 *Chaos Solitons Fractals* **5** 461
[65] Kuva S M, Lima G F, Kinouchi O, Tragtenberg M H and Roque A C 2001 *Neurocomputing* **38–40** 255